Supporting Information for

Highlightable Ca^{2+} Indicators for Live Cell Imaging

Hiofan Hoi[†], Tomoki Matsuda[‡], Takeharu Nagai[‡], Robert E. Campbell[*,†]

[†]Department of Chemistry, University of Alberta, Edmonton, Alberta T6G 2G2, Canada. [‡]Department of Biomolecular Science and Engineering, The Institute of Scientific and Industrial Research, Osaka University, Mihogaoka 8-1, Ibaraki, Osaka 567-0047, Japan.

Correspondence should be addressed to R.E.C. (robert.e.campbell@ualberta.ca)

This document contains:

Supporting Results and Discussion

Attempted development of a photoactivatable GECO based on paGFP and G-GECOs. Wild-type GFP (wtGFP) undergoes photoactivation (an increase in green fluorescence when excited at 475 nm) when irradiated with UV or ~400 nm light.[1] The chromophore of wtGFP exists in an equilibrium between the neutral phenol state (abs_{max} = 397 nm) and the anionic phenolate state (abs_{max} = 475 nm). Absorbance by either state results in green fluorescence. However, illumination with UV or ~400 nm light can also lead to decarboxylation of Glu222 (albeit with a lower quantum efficiency) and a rearrangement of the hydrogen-bond network that shifts the chromophore equilibrium towards the phenolate state.[2,3] With the goal of improving the contrast of this photoactivation and creating a useful FP-based highlighter, Patterson and colleagues screened a library of mutations at position 203. This effort led to the identification of the T203H variant of GFP that has a more than 100× increase in green emission with 488 nm when photoactivated with ~ 400 nm light.[4] We introduced the analogous V116H mutation (G-CaMP numbering) into green-emissive GECOs, namely G-GECO1.1-1.3, GEM-GECO1 and GEX-GECO1. The V116H variants of G-GECO1.1-1.3 variants retained strong green fluorescence with 480 nm excitation and no photoactivation was observed after illuminated with 400 nm in *E. coli* colonies. For GEX-GECO1, V116H substantially diminished its brightness, and abolished its Ca^{2+} response. GEM-GECO with V116H had an inverted Ca^{2+} response at ~515 nm when excited at ~ 400 nm. Neither GEX- nor GEM-GECO1 underwent photoactivation even with prolonged photoactivation (26 min). Position 116 (i.e., position 203 in GFP numbering) is located at the interface between the cpGFP and calmodulin in G-CaMP and a threonine at this position was found to participate in a hydrogen bond network which stabilizes the ionized state of the chromophore.[5] Substitution of threonine with valine was introduced during the evolution from G-CaMP2 to G-CaMP3.[6] We suspect that, in contrast to PA-GFP where the Thr203His mutation stabilizes the neutral chromophore,[7] this substitution is stabilizing the anionic form of the chromophore in the context of the G-GECOs.

The E222Q mutation has been reported to make avGFP and its derived variants reversibly photoswitchable.[8] Introduction of the analogous mutation into GEX- and GEM-GECO1 did not introduce an analogous property. No recovery of green fluorescence was observed following photobleaching by illumination with 480 nm light.

Attempted development of a photoactivatable GECO based on pamCherry and R-GECO. R-GECO1 is a red-emissive GECO based on circularly permuted mApple.[9] Since mApple and mCherry are both derived from *Discosoma* RFP,[10] and mCherry has been converted into the photoactivable variant pamCherry,[11] we hypothesized that introducing mutations responsible for the photoactivation behavior of pamCherry into R-GECO1 might generate a photoactivable red fluorescent GECO. It has been proposed the pamCherry initially forms a non-coplanar chromophore structure that lacks the C^{α}-C^{β} double bond at Tyr67 that is present in the normal mCherry chromophore.[12] Irradiation promotes the oxidation of the C^{α}-C^{β} of the Tyr67 of the chromophore through a mechanism that involves the decarboxylation of Glu215. Mutagenesis studies indicated that Lys70Asn and Ile197Arg are minimally required to the photoactivation. Accordingly, we targeted the equivalent residues in R-GECO, and several others thought to be important for photoactivation (i.e., V148, I165, K167, and L169) for generation of semi-saturation libraries. Libraries were screened in *E. coli* colonies for both photoactivation and Ca^{2+} responses. Several mutants that exhibited photoactivation behavior upon 400 nm light irradiation were identified. Of them, R-GECO-V148M/I165V/K167A, designated as paR-GECO0.1, exhibited the best, though still modest, photocontrast (6-fold). Notably, mutations at Lys70 and Ile197 were not required to make R-GECO photoactivable. paR-GECO0.1 has a single absorbance peak at 402 nm in the visible spectrum range (Figure S1). Irradiation with ~400 nm light generates a new absorbance peak at 565 nm, which emits maximally at 605 nm. Unfortunately, paR-GECO0.1 and other less photoactivable mutants showed only subtle Ca^{2+} responses (15~30% $\Delta F/F_{min}$) in stark contrast to the 16-fold change of R-GECO1. Assuming that the photoactivation mechanism of paR-GECO0.1 is similar to that of pamCherry, the post-photoactivated chromophore would be the *trans* isomer and therefore oriented differently than the *cis* chromophore of mApple and mCherry.[12] Accordingly, the phenolate group of the paR-GECO0.1 chromophore will not be positioned to engage in the key interactions with CaM that give rise to the large fluorescence change of R-GECO1. Discouraged by the modest photocontrast and poor Ca^{2+} response, and also concerned about the isomeric form of the chromophore, we did not pursue further directed evolution on paR-GECOs. It is possible that additional directed evolution and engineering could potentially lead to the development of useful imaging tools based on these variants.

Materials and Methods

General methods and materials. All synthetic DNA oligonucleotides for cloning and library construction were purchased from Integrated DNA Technologies (Coralville, IA). Restriction enzymes were purchased from New England Biolabs or Fermentas and used according to the manufacturer's recommended protocol. Taq (New England Biolabs) and Pfu polymerases (Fermentas) were used for error-prone PCR or regular PCR, respectively. PCR products and products of restriction digests were purified using GeneJET gel extraction kit (Fermentas) according to the manufacturer's protocols. The cDNA sequences were confirmed by dye terminator cycle sequencing using the BigDye Terminator v3.1 Cycle Sequencing Kit (Applied Biosystems). Sequencing reactions were analyzed at the University of Alberta Molecular Biology Service Unit.

Generation of circularly permuted variants of mMaple. Overlap extension PCR was used to generate circularly permuted variants of mMaple. For example, to generate the cpmMaple193 variant, cDNA encoding residues 193-232 was amplified using a 5' primer with a *XhoI* site and a 3' primer with an overhang encoding "GGSGG". In parallel, the cDNA encoding residues 1-193 was amplified using a 5' primer with a complementary sequence encoding "GGSGG" and a 3' primer with two extra Gly residues followed by an *EcoRI* site. The terminal residues (i.e., positions 193 and 192) were randomized with an NNK sequence that encodes for all 20 amino acids using 32 codons. The above two fragments were then stitched together by overlap extension PCR to generate cpmMaple193. CpmMaple207, 145, 140, 143 and 144 were constructed by similar methods, except that the last three constructs had only one extra glycine residue at the new C-terminus. The assembled cDNA was digested with *XhoI* and *EcoRI* and ligated into similarly digested pBAD/His B (Invitrogen). Electrocompetent *Escherichia coli* strain DH10B (Invitrogen) was transformed by electroporation and plated on LB (Luria–Bertani)/agar plates supplemented with ampicillin (0.1 mg/ml) and L-arabinose (0.02%). Plates were incubated overnight at 37°C and then at room temperature prior to screening.

Plasmid library creation and site-directed mutagenesis of GR-GECOs and other pa-GECOs. Linker libraries of GR-GECOs were generated by amplifying the cDNA of cpmMaple145 with various 5' primers with an *XhoI* site and 3' primers with a *MluI* site. These primers encode for polypeptide sequence that starts or stops at various positions between residues

141 to 147. The purified PCR products were digested with *XhoI* and *MluI* and ligated into similarly digested pTorPE. The pTorPE is a modified pBAD/His B contains a TorA periplasmic export sequence ahead of the 6×His tag.[9]

Randomly mutated libraries were created by error prone PCR,[13] using a 5' primer with an *XbaI* site annealing to the 6×His tag and a 3' primer with a *HindIII* site. In addition, a modified staggered extension process (StEP) PCR was used to create libraries that contained various combinations of beneficial mutations found during previous rounds of screening.[14] Briefly, a total of 0.1 pmol pBAD/His B plasmids, containing the genes for 5-15 different GR-GECO variants selected from randomly mutated libraries, were used as the template mix. The mixture was PCR amplified for 80-100 short cycles (94°C for 20 s, 55°C for 15 s and then 72°C for 5 s), followed by a final extension step at 72°C for 5 min.

Saturation or semi-saturation mutagenesis at specific residues was performed using overlap extension PCR or QuickChange Site-Directed Mutagenesis Kit (Agilent Technologies). Regardless of library assembly method (i.e., error prone PCR, saturation mutagenesis, or StEP PCR), gene libraries were digested with *XbaI* and *HindIII* and inserted into a similarly digested pTorPE. Electrocompetent *E. coli* strain DH10B (Invitrogen) was transformed and plated on LB (Luria–Bertani)/agar plates supplemented with ampicillin (0.1 mg/ml) and L-arabinose (0.0004-0.0008%). Plates were incubated overnight at 37°C and another 10-24 hours at room temperature prior to screening.

Plasmid library screening. Since the expressed protein was exported to the high Ca^{2+} environment of the periplasm, colonies containing functioning Ca^{2+} sensors would, in principle, manifest brighter fluorescence. To screen for both photoconversion (or photoactivation) and Ca^{2+} response, we performed a two-step screening procedure. In the first step, plates containing colonies were photoactivated or photoconverted for 5-15 min using a custom built illumination source composed of six 9 × 11 arrays of 405 nm light emitting diodes (LED) (OptoDiode Corporation, Newbury Park, CA). The light intensity at the colony plane was 17.6 mW/cm^2 as measured with a light power meter (PowerMax 5100, Molectron Incoporated, Portland, OR). Colonies exhibiting the brightest fluorescence in the post-photoactivation/photoconversion channel were selected. For directed evolution of GR-GECOs, the bright red fluorescence could be result of either high photoconversion or high Ca^{2+} response, or both. To ensure the selected

variants had satisfactory Ca^{2+} response, they were grown at 37°C overnight in LB media supplemented with ampicillin and L-arabinose, then transferred to 30°C for another 10-24 hr. Cells were pelleted by centrifuge, washed with a $MgSO_4$/EGTA solution to remove excess Ca^{2+}, and lysed in B-PER (Pierce). A portion of this B-PER lysate was taken out for spectrofluorometric testing of the Ca^{2+} response of the green species. The remainder of the lysate was photoconverted using the aforementioned chamber. Both the pre- or post- photoconversion proteins were diluted into KCl-MOPS buffer (30 mM MOPS, 100 mM KCl, pH 7.4) in a 96-well plate for Ca^{2+} response test. Three fluorescence intensities was recorded for each sample: the initial value (F_{ini}), the value after addition of 0.4 mM (final concentration) EGTA (F_{EGTA}), and the value after addition of equivalent amount of Ca^{2+} ($F_{Ca^{2+}}$). Variants showing the largest ($F_{Ca^{2+}}$-F_{EGTA})/F_{EGTA} ($\Delta F/F_{min}$) value were considered as winners. Plasmids for these variants were extracted for sequencing and served as templates for subsequent library generation.

Protein purification and characterization. Protein purification was carried out as previously described.[15] The buffer was changed into PBS (pH 7.4) for cpmMaple variants or KCl-MOPS buffer (30 mM MOPS, 100 mM KCl, pH7.4) for GR-GECOs. All absorption measurements were acquired on a DU-800 UV–visible spectrophotometer (Beckman). Unless otherwise indicated, all fluorescence spectra were recorded on a QuantaMaster spectrofluorometer (Photon Technology International) and have been corrected for the detector response. For protein samples representative of the apo state (i.e., Ca^{2+} free state), concentrated protein sample was diluted into Ca^{2+} free KCl-MOPS buffer (30 mM MOPS, 100 mM KCl and 4 mM EGTA, pH7.4). For protein samples representative of the saturated state (i.e., Ca^{2+} bound sate), concentrated protein was diluted into Ca^{2+} containing KCl-MOPS buffer (30 mM MOPS, 100 mM KCl and 4 mM $CaCl_2$, pH7.4). To obtain the red state of the GR-GECOs, concentrated protein was subjected to illumination with the custom built 405 nm light source for 10 min.

Molar extinction coefficients (ε) and quantum yields (Φ) determination. Molar extinction coefficients (ε) for the green states were measured by the alkali denaturation method.[16,17] Briefly, the protein was diluted into regular buffer or 0.01 M NaOH and the absorbance spectra recorded under both conditions. The ε was calculated as: $\varepsilon = (Abs_{sample}/Abs_{\mathrm{den},445})\times\varepsilon_{den,445}$, where $\varepsilon_{den,445}$ is 44,000 M^{-1} cm^{-1}. To determine ε for the red state, the green state protein absorbance was recorded and the sample was then photoconverted until the absorbance peak of the red

species reached a plateau. The ε of the green state was used as reference to calculate that of the red states. To determine the fluorescence quantum yields (Φ), purified proteins were diluted into citrate-borate buffer (pH 9.0) with 4 mM EGTA or with 4 mM Ca^{2+}. The high pH buffer was used in order to yield enough absorbance and emission of the deprotonated state at low protein concentration. Fluorescein in 10 mM NaOH (Φ = 0.95),[18] and the red species of mMaple in PBS (pH 7.4) (Φ = 0.53), were used as Φ standards for the green and red states, respectively.

Ca^{2+} titration for K_d determination. To determine the K_d of GR-GECOs for binding to Ca^{2+}, a series of KCl-MOPS buffers containing different amount of Ca^{2+} were prepared following the instructions provided in the Calcium Calibration Buffer Kit (Invitrogen). Purified GR-GECOs was then diluted 1:100 into the Ca^{2+} buffer and their fluorescence measured with a Safire2 plate reader (Tecan). Data was fit with a Hill equation: $F_i = F_0 + (F_{max} - F_0) \times \frac{[Ca^{2+}]^n}{(K_d{}^n + [Ca^{2+}]^n)}$, where n is the Hill coefficient and F_0 and F_{max} are the fluorescence without Ca^{2+} and with saturated Ca^{2+}, respectively. The calculated K_d represents the concentration of Ca^{2+} when the fluorescence change of the indicator is half of its maximum value.

pH titration for pK_a determination. For determination of the pH dependence, concentrated GR-GECO proteins were diluted 1:50 into a series of pH-adjusted borate/citrate buffers with 4 mM EGTA or 4 mM $CaCl_2$ in a 96-well black clear bottom plate (Corning). Fluorescence was measured using a Safire2 plate reader.

Stopped-flow spectroscopy for Ca^{2+}-binding kinetics determination. A SX20 stopped-flow spectrometer (Applied Photophysics) equipped with a 150 W xenon lamp and a fluorescence photomultiplier was used for stopped flow kinetic measurements. The GR-GECO indicator (in 30 mM MOPs, 1 mM EGTA and 100 mM KCl) was rapidly mixed (1:1) with a series of Ca^{2+} buffers. Excitation wavelength was set to 480 nm for the green and 525 nm for red species, each with a slit width of 14 nm. A 535/50 nm filter (for green emission) and a 585/40 nm filter (for red emission) were used. The change in the fluorescence signal during rapid mixing provided the relaxation rate constants (k_{obs}) for the Ca^{2+} association reaction at various Ca^{2+} concentrations (from 60 nM to 500 nM). By fitting the observed data to the equation $k_{obs} = k_{on} \times [Ca^{2+}]^n + k_{off}$, the kinetic constants of Ca^{2+} association k_{on} and dissociation k_{off} were determined.

Photoconversion with and without Ca^{2+}. Purified protein was diluted into KCl-MOPS buffer with 4 mM EGTA or with 4 mM Ca^{2+} and subsequently photoconverted into the red sate using

the 405 nm LED. Absorbance spectra at different photoconversion times were recorded. Notably, prolonged photoconversion of GR-GECOs depletes their Ca^{2+}-responding capability, possibly due to photoinduced or singlet-oxygen dependent modifications of the protein residues.

Mammalian expression vectors. To create the GR-GECO cytoplasmic expression vectors, the gene was amplified with a 5' primer with a *BamHI* site and a 3' primer with an *EcoRI* site. The purified PCR products were digested and ligated into a similarly digested modified pcDNA3 plasmid.[9] Briefly, this modified pcDNA3 plasmid was made by deleting 2224 nucleotides (including the SV40 promoter, the SV40 origin of replication, the Neomycin ORF, and the SV40 poly A region) from the original 5.4 kb pcDNA3 (Invitrogen).

To create the nucleus-localized GR-GECOs for photobleaching, the gene was amplified with a 5' primer with a *XhoI* site and a 3' primer with an *BamHI* site. The digested gene was ligated into another modified pcDNA3.1 that had been digested with the same two restriction enzymes. This modified pcDNA3.1 has altered restriction sites compared with the original pcDNA3.1 (Invitrogen) and an in-frame nucleus localization signal (NLS) peptide comprised of three repeated copies of "DPKKKRKV" at the C- terminal end of the cloning site.

Cell culture and transfection. HeLa cells (CCL2 line; ATCC) were maintained in Dulbecco's Modified Eagle Medium (DMEM) (Invitrogen) supplemented with 10% fetal bovine serum (FBS) (Sigma), 2 mM GlutaMax (Invitrogen) and penicillin-streptomycin. Plasmids for transfection were prepared using the GeneJET™ Plasmid Miniprep Kit (Fermentas). Transfection was carried using TurboFect™ (Fermentas) according to the manufacturer's protocol.

Dissociated hippocampal neurons were prepared at embryonic day 18, and were grown on a homemade 35-mm glass bottom dish containing MEM with 2% B27 Supplement (GIBCO), 2 mM glutamine, 1 mM sodium pyruvate (GIBCO), penicillin-G potassium salt (50 units/mL), and streptomycin sulfate (50 μg/mL). On the 4th day in vitro (DIV-4), half of the culture medium was replaced with MEM containing 2% FBS, 1 × N2 Supplement (Invitrogen), and penicillin-streptomycin. Neuronal cells were transfected at DIV-7 by using calcium phosphate precipitation. Cells were imaged 2-4 days after transfection

Live cell imaging. Imaging was done 36~48 h after transfection. The culture medium was changed to HEPES (25 mM) buffered Hanks' Balanced Salt Solution (HBSS) before imaging. An

inverted Nikon Eclipse Ti microscope equipped with a 75 W mercury-xenon lamp (Hamamatsu), 20× and 40× objectives (Nikon), and a 16-bit QuantEM 512SC electron-multiplying CCD (Photometrics) was used to perform standard Ca^{2+} calibration experiment. Photoconversion was done using the epi-fluorescence illumination source and a DAPI excitation filter set (335-385 nm with a 400 nm dichroic). The following filter sets were used for imaging: 483-493 nm (exciation), 500-550 nm (emission), and 488 nm (dichroic) for the green channel; 538-548 nm (excitation), 563-637 nm (emission), and 543 nm (dichroic) for the red channel.

For time-lapse imaging experiments, 5 μM (final concentration) histamine was added into the cell culture to induce [Ca^{2+}] fluctuations in the cytoplasm. The cytoplasmic Ca^{2+} was then depleted by addition of 4 mM EGTA and 5 μM ionomycin to deplete intracellular Ca^{2+} and shift the indicators to the apo-state. In a final step, 10 mM $CaCl_2$ and 5 μM ionomycin were applied to determine the maximum fluorescence signal with indicators fully saturated with Ca^{2+}. To examine the photobleaching behavior, transfected HeLa cells expressing GR-GECOs targeted to the nucleus were identified at the lowest possible excitation intensity. Identified cells were then subjected to constant illumination at the full power of the 75 W mercury-xenon lamp, and the intensity of the fluorescence recorded as a function of time.

For the single cell highlighting and Ca^{2+} imaging experiment, a Nikon Eclipse equipped with same camera and lamp, a 60× oil-immersion Apo TIRF objective (NA 1.49) (Nikon), and a 408 nm photoactivation laser with a power of >500 mW (Melles Griot) was used. The photoactivation laser delivers a spot illumination with an approximate diameter of 14.3 μm at the center of the field of view and a measured intensity of 187 μW. As the laser power at the focal point varies between microscope setups, it is likely that both photoactivation power and duration will need to be optimized on other imaging systems. As we intended to measure Ca^{2+} response at both green channel and red channel, we typically photoconverted approximate half of the GR-GECO protein into the red form. The following filters were used: 465-495 nm (excitation), 515-555 nm (emission), and 505 nm (dichroic) for the green channel; 528-553 nm (excitation), 590-650 nm (emission), and 565 nm (dichroic) for the red channel. Image procession was done using ImageJ. For imaging of dissociated hippocampal neurons, an Olympus confocal inverted microscope FV1000 equipped with UPLSAPO 60 × 1.35 numerical aperture (NA) oil objective and multi-argon ion laser was used. Images of green and red fluorescence signals were detected

at 500-535 nm and 555-655 nm wavelength range, respectively, using 488 nm excitation. A 25 mW 405 nm laser diode at 12% power was used for photoconversion.

Supporting Figures

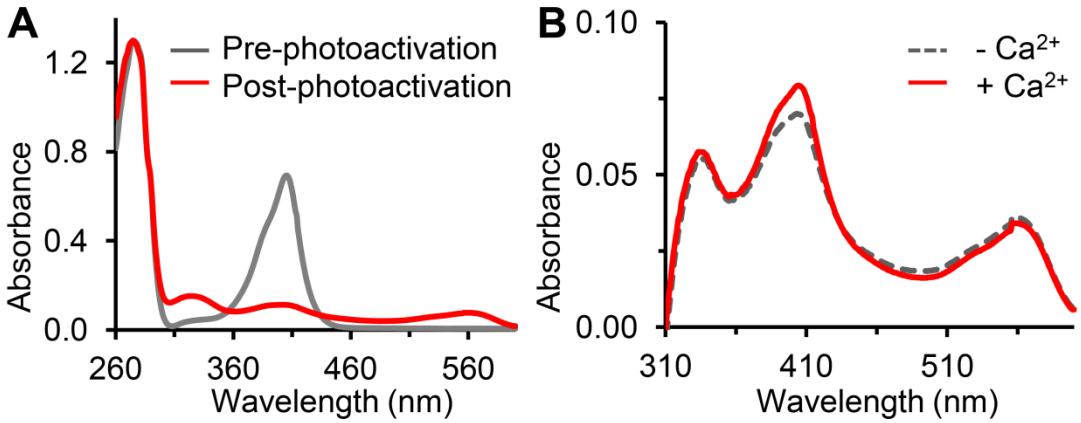

Figure S1. Absorbance spectra of paR-GECO0.1. (A) Absorbance spectra before and after 16 min illumination with 405 nm LED light. paR-GECO0.1 has a major absorbance peak at 400 nm which is dimly blue fluorescent and could be photoconverted into red. (B) Absorbance spectra of the post-photoactivation species with and without Ca^{2+}.

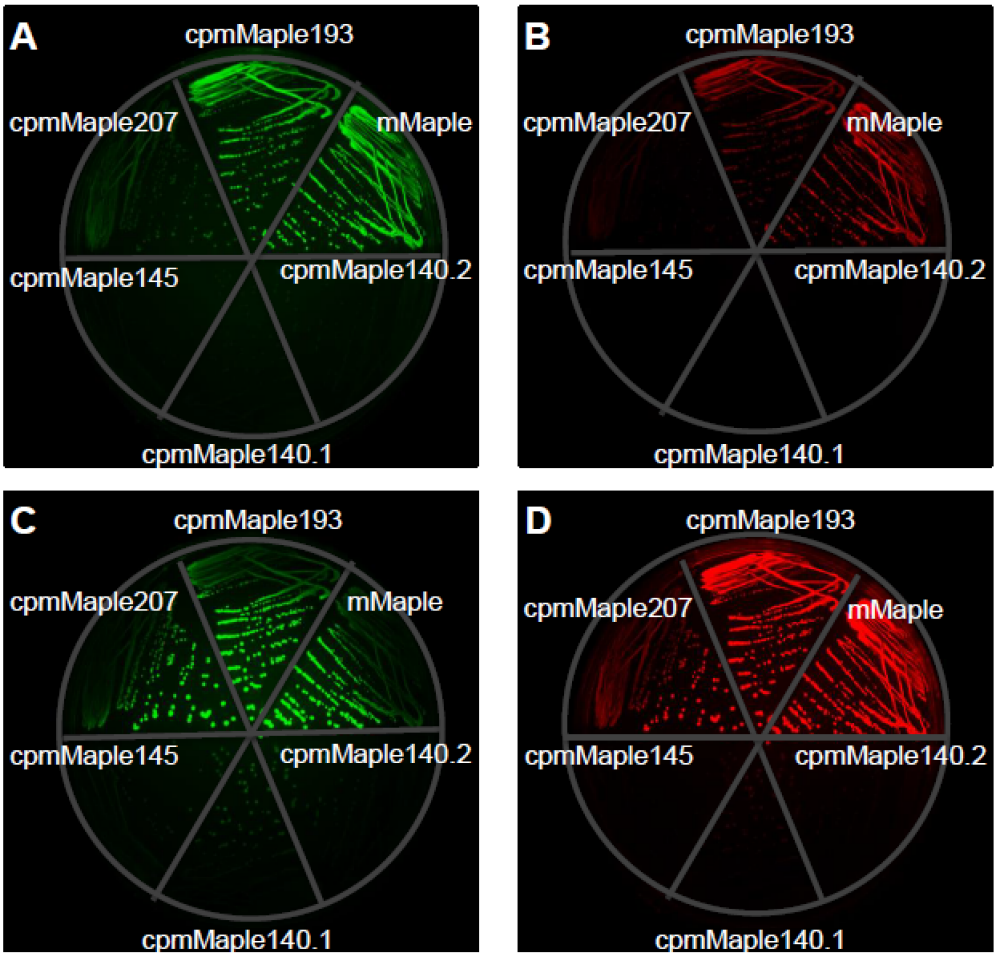

Figure S2. Fluorescent images of *E. coli* expressing cpmMaple variants on a Petri dish. (A-B) Pre- (A) and post-photoconversion (B) images of *E. coli* grown for 15 hours at 37°C. (C-D) Green (C) and red (D) fluorescence of the same plate after another 5-days at room temperature. Additional photoconversion was used to convert newly synthesized FPs to red before acquisition of (D). Substitution at the new N- and C- termini are His and Asp for cpmMaple193, Arg and stop codon for cpmMaple207, Gly and Thr for cpmMaple145, Thr and stop codon for cpmMaple140.1 and Asp and Ala for cpmMaple140.2.

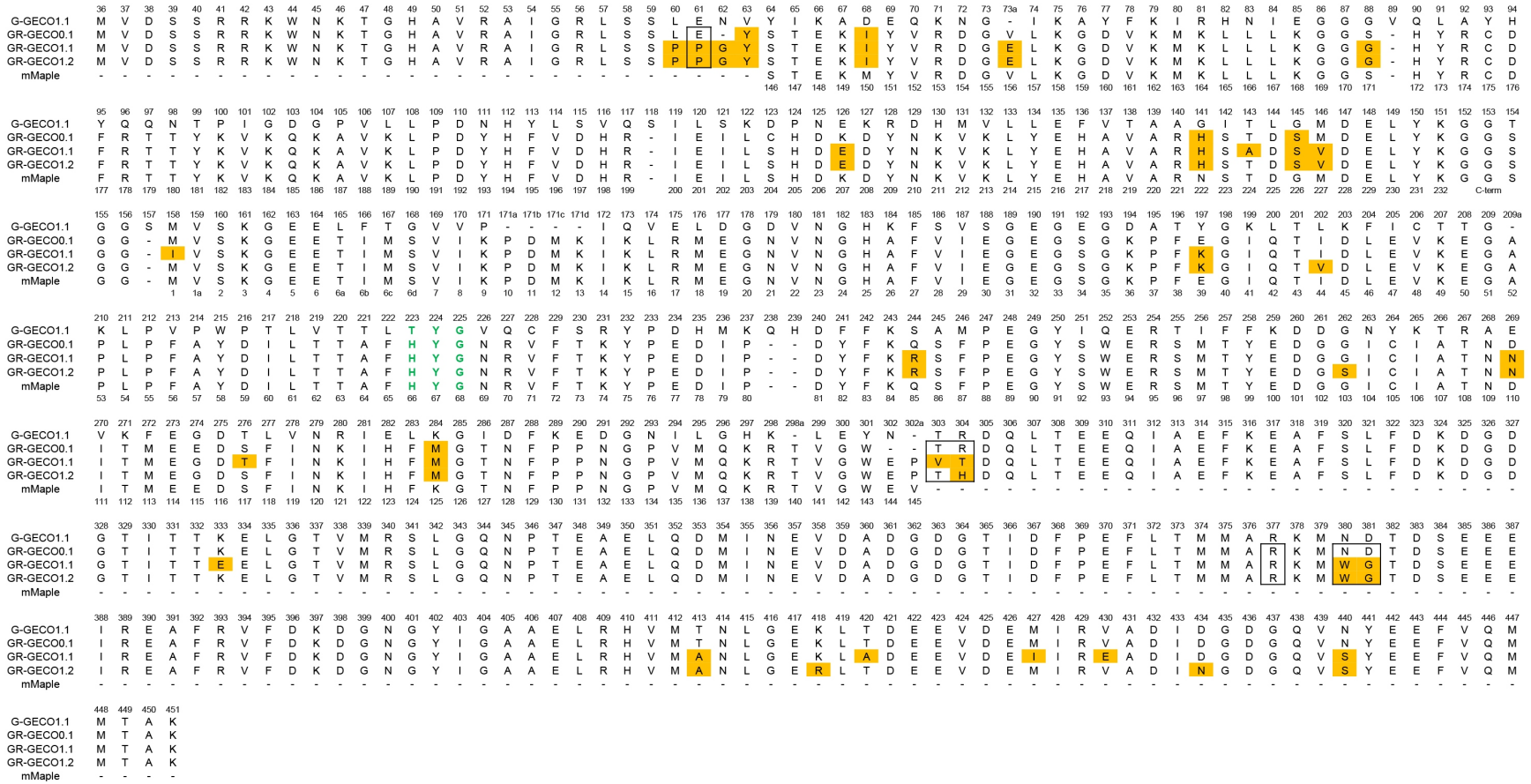

Figure S3. Sequence alignment of GR-GECOs, G-GECO1.1 and mMaple. Positions targeted for saturation or semi-saturation mutagenesis are highlighted with a box. Mutations found are highlighted with orange shade. Letters in green are the chromophore forming residues. Top row numbering corresponds to G-CaMP and G-GECO numbering convention. Bottom row numbering corresponds to mMaple numbering convention.

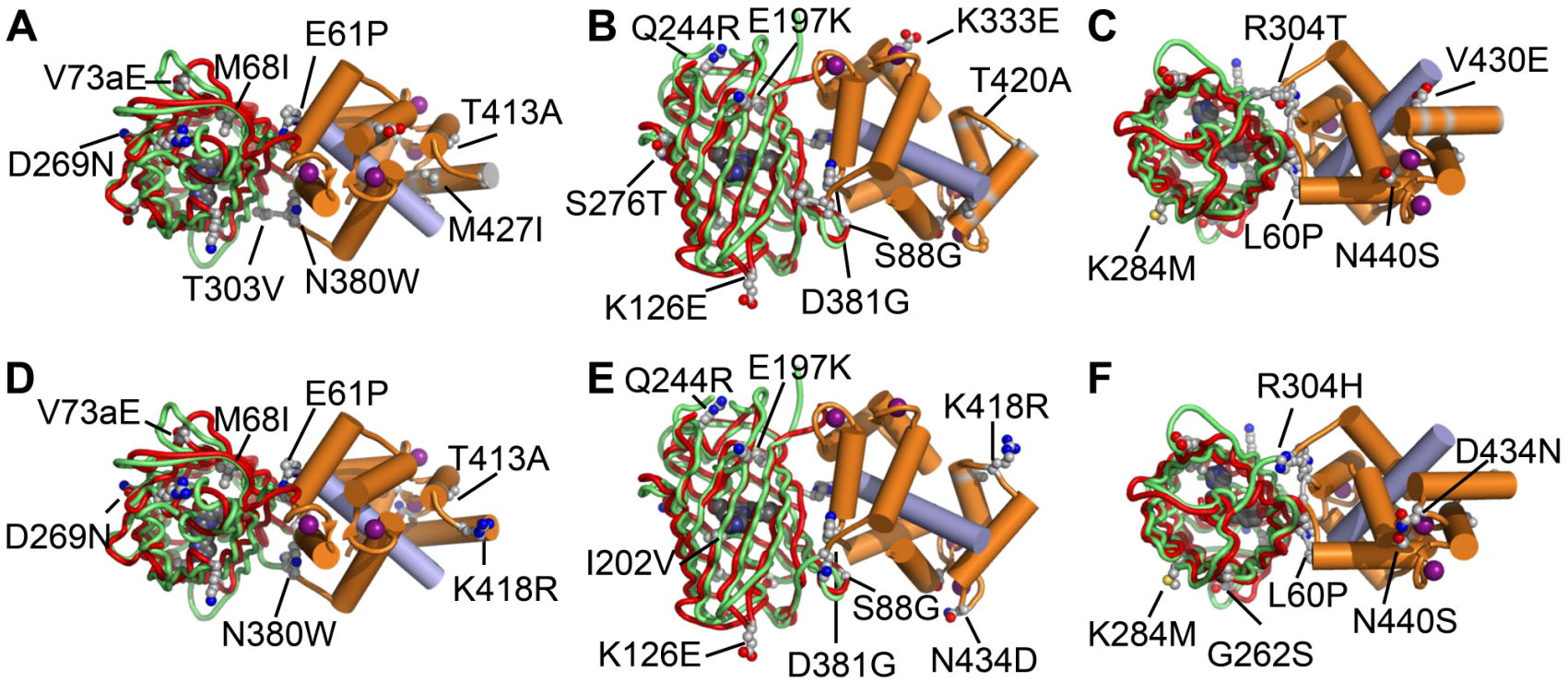

Figure S4. Location of substitutions in GR-GECOs. Structure of G-CaMP2 (PDB: 3EVR) and the pre-photoconversion state of Eos (PDB: 1ZUX), a photoconvertible FP that is a close homolog of mMaple, are aligned to represent the overall structure of GR-GECOs.[19,20] Structure of cpGFP in G-CaMP2 is represented in green, while structure of Eos is represented in red. (A-C) Top (A), side (B) and bottom (C) views of GR-GECO1.1. Substitutions not shown in the picture includes 2+62G, 1+63Y, N141H, T143A, G145S, M146V and M158I. "+" means extra residues before cpmMaple (Figure S3). (D-F) Top (D), side (E) and bottom (F) views of GR-GECO1.2. Substitutions not shown in the picture includes 2+62G, 1+63Y, N141H, G145S and M146V (Figure S3).

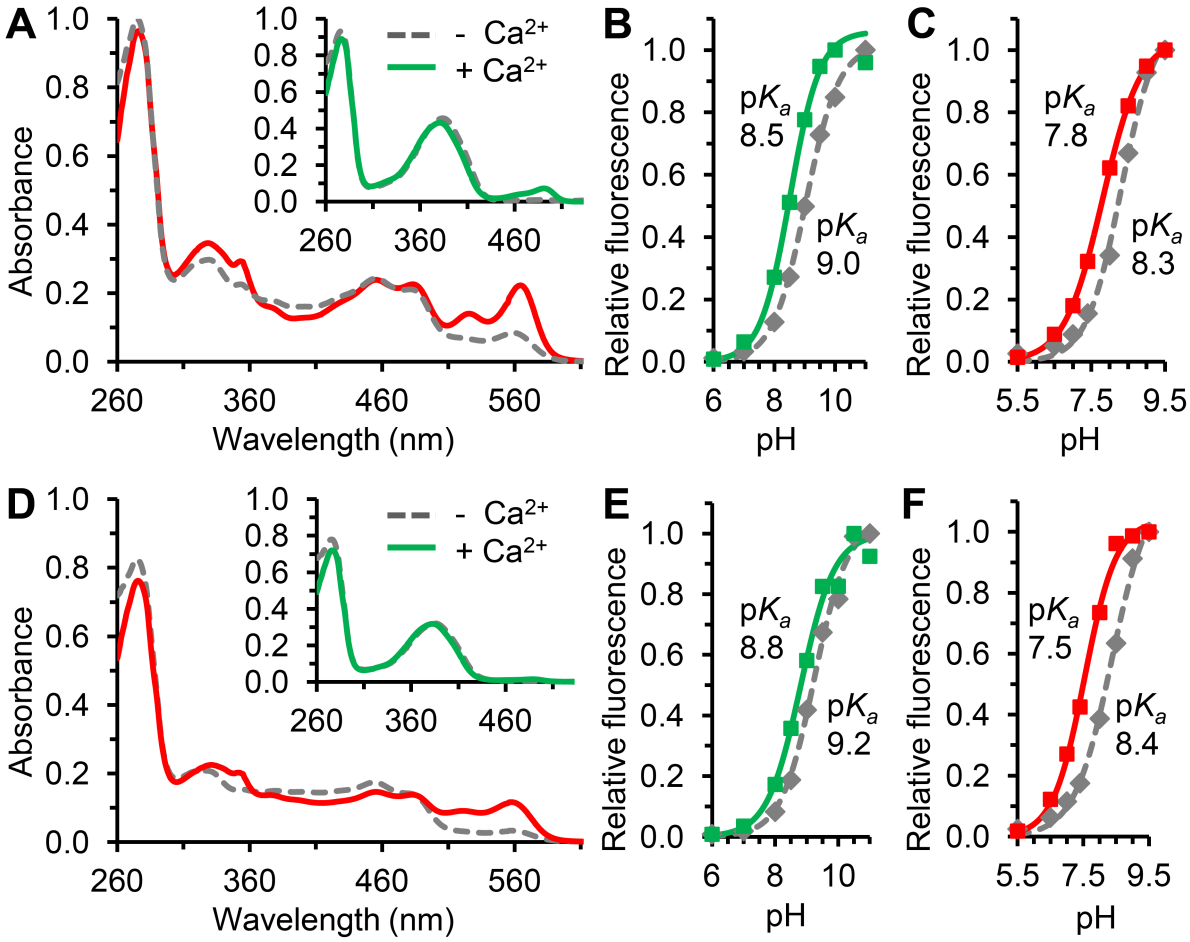

Figure S5. Absorbance spectra and pH titration of GR-GECOs. (A) Absorbance spectra of the red and green (inset) species of GR-GECO1.1 with (solid red or green) and without (dashed grey) Ca^{2+}. (B-C) pH titration of the green (B) and the red (C) species of GR-GECO1.1 with (green or red square) or without (grey diamond) Ca^{2+}. (D) Absorbance spectra of the red and green (inset) GR-GECO1.2 with (solid red or green) and without (dashed grey) Ca^{2+}. (E-F) pH titration of the green (E) and red (F) species of GR-GECO1.2 with (green or red square) and without (grey diamond) Ca^{2+}.

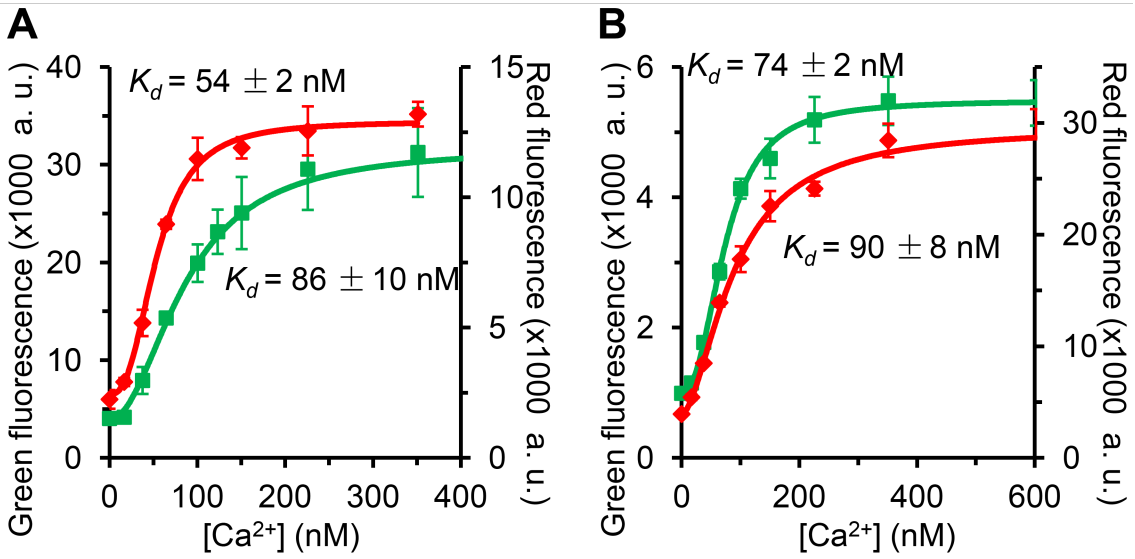

Figure S6. Ca^{2+} titration of GR-GECOs. (A-B) Fluorescence intensity plotted as a function of the $[Ca^{2+}]$ for the green (green square) and red species (red diamond) of GR-GECO1.1 (A) and GR-GECO1.2 (B). K_d and Hill coefficients are determined by fitting to the equation $F_i = F_0 + (F_{max} - F_0) \times \frac{[Ca^{2+}]^n}{(K_d{}^n + [Ca^{2+}]^n)}$.

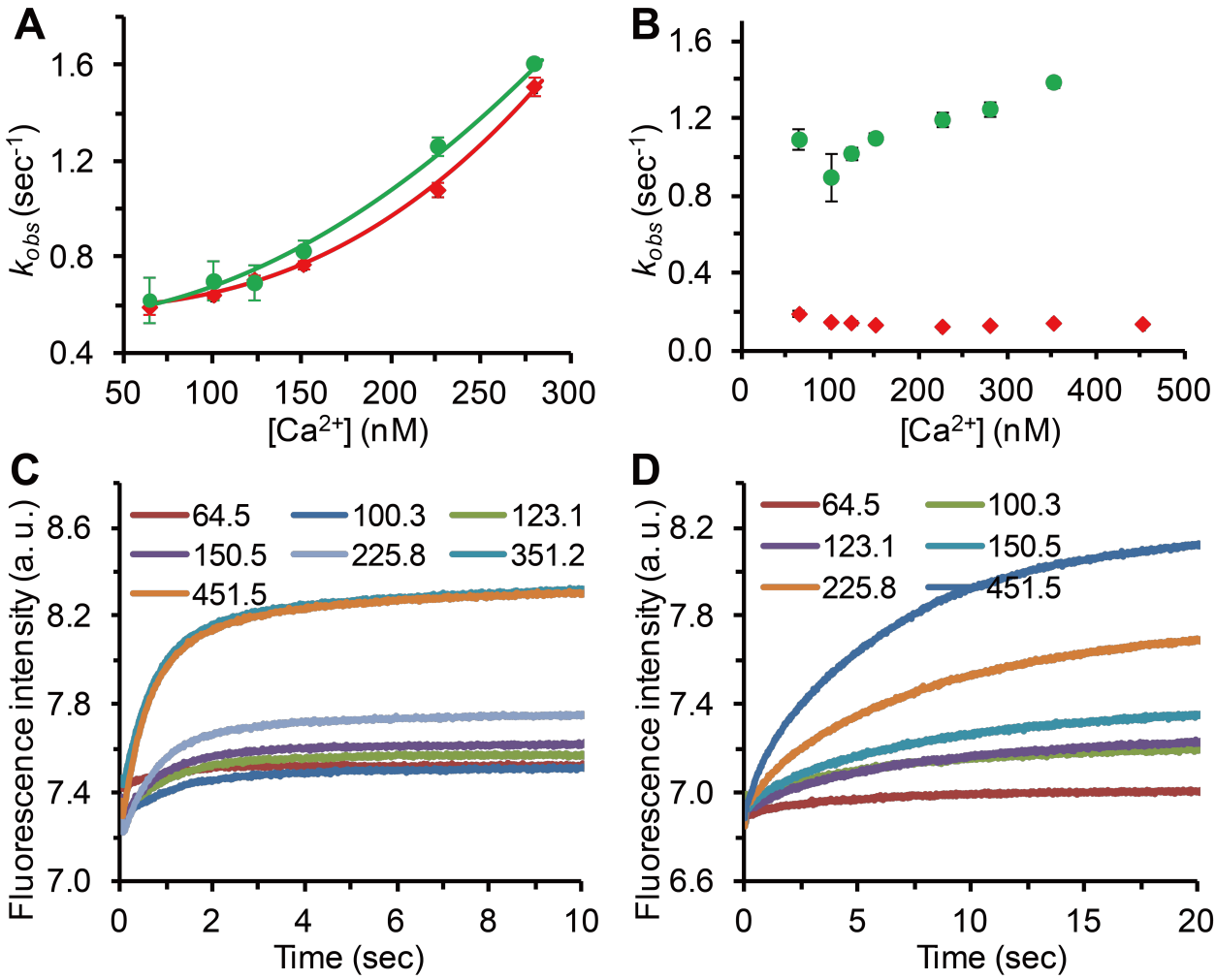

Figure S7. Stopped-flow kinetic characterization of GR-GECOs. (A-B) Observed relaxation rate constants (k_{obs}) plotted as a function of [Ca^{2+}] for both green (green circle) and red species (red diamond) of GR-GECO1.1 (A) and GR-GECO1.2 (B). Association (k_{on}) and dissociation (k_{off}) rate constants of GR-GECO1.1 were determined by fitting to the equation $k_{obs} = k_{on}[Ca^{2+}]^n + k_{off}$. Values are tabulated in Table S5. Data for GR-GECO1.2 could not be satisfactorily fit using the same procedure, suggesting that the binding kinetics are more complex for this variant. (C-D) Relaxation trace of the green species (C) and the red species (D) of GR-GECO1.2. Numbers in the legend are the [Ca^{2+}] in nM.

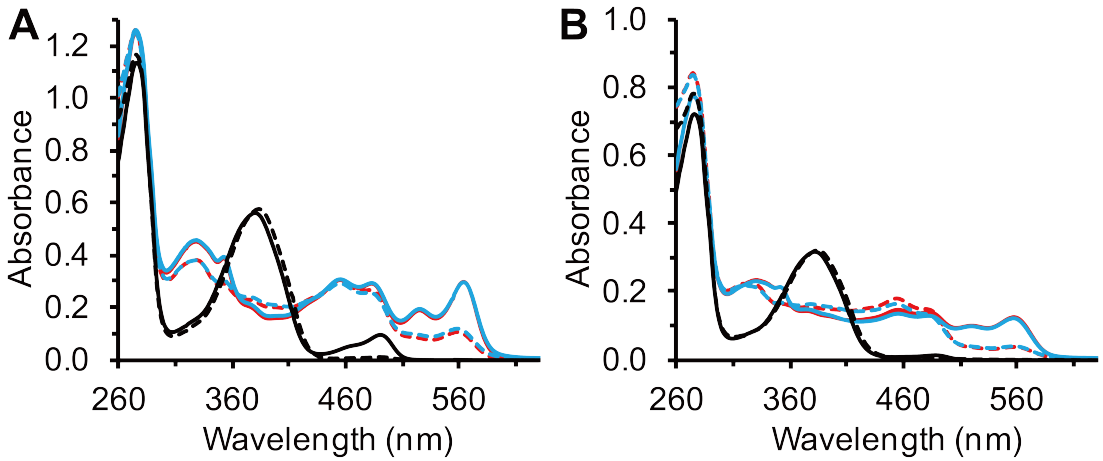

Figure S8. Effect of 460 nm illumination on photoswitching. Absorbance spectra of GR-GECO1.1 (A) and GR-GECO1.2 (B) before photoconversion (black), after 30 min illumination with 400 nm LED (red) and after another 30 min illumination with 460 nm LED (blue). The Ca^{2+} free states are represented by dashed lines, while the Ca^{2+}-bound states are represented by solid lines. Unlike mMaple,[21] the red species of GR-GECOs do not undergo observable photoswitching with prolonged illumination at 460 nm.

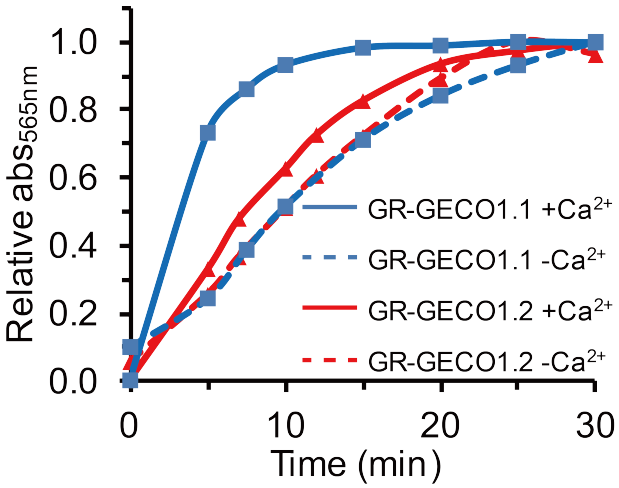

Figure S9. Photoconversion profile of GR-GECOs. The 405 nm LED illumination system was used for photoconversion. Photoconversion of GR-GECO1.1, as monitored as the generation of the red anionic state (i.e., absorbance at 565 nm), is faster than that of GR-GECO1.2.

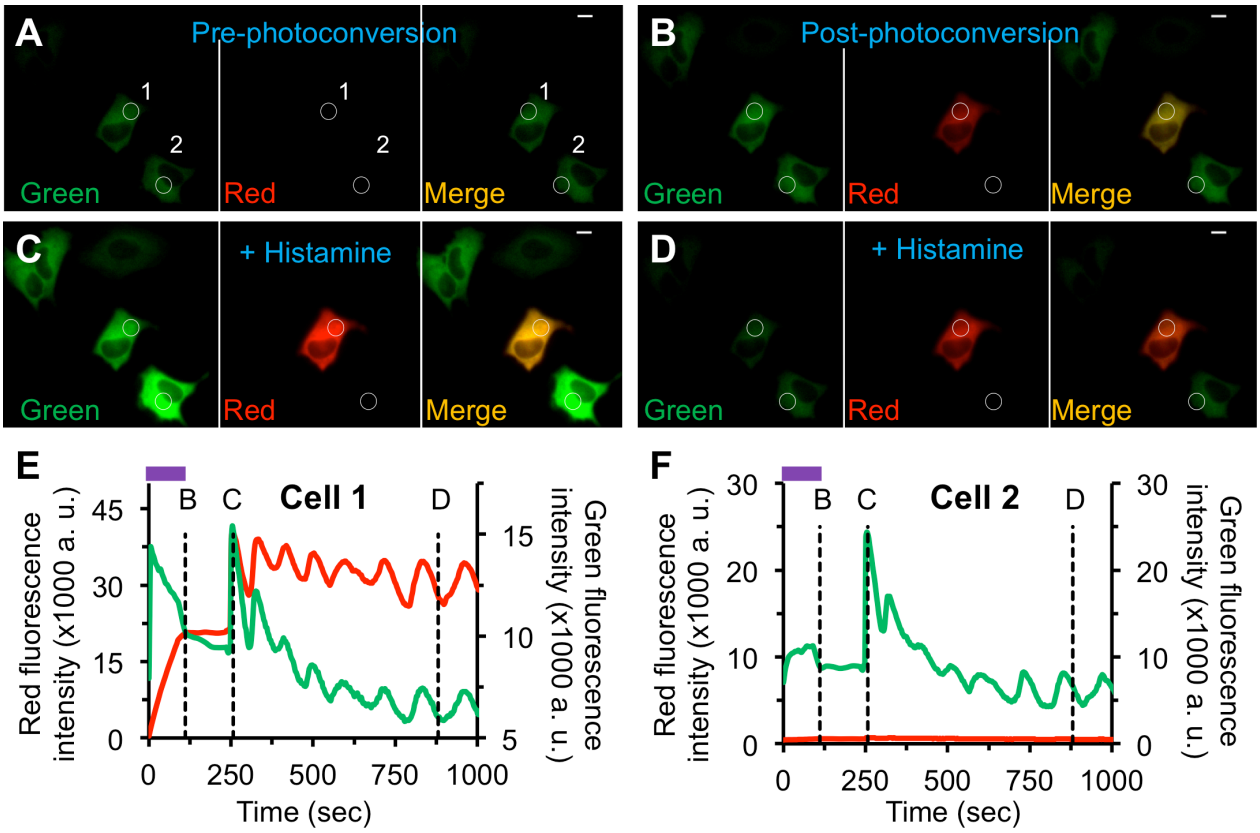

Figure S10. Imaging histamine-induced Ca^{2+} oscillations in highlighted HeLa cells. (A-D) Fluorescence images of HeLa cells expressing GR-GECO1.1: (A) before photoconversion; (B) after 90 sec of photoconversion of cell 1; (C) immediately after the addition of 5 μM histamine; and (D) during Ca^{2+} oscillations. For panels A-D, the left, center, and right images are the green fluorescence, red fluorescence, and merged channels, respectively. Scale bar 10 μm. (E) Fluorescence intensity plotted as a function of time for cell 1. Times points for the images in panels B-D are indicated with a dashed vertical line. Purple bar indicates the duration of photoconversion (90 sec). (F) Fluorescence intensity plotted as a function of time for cell 2. Images taken from Movie S1.

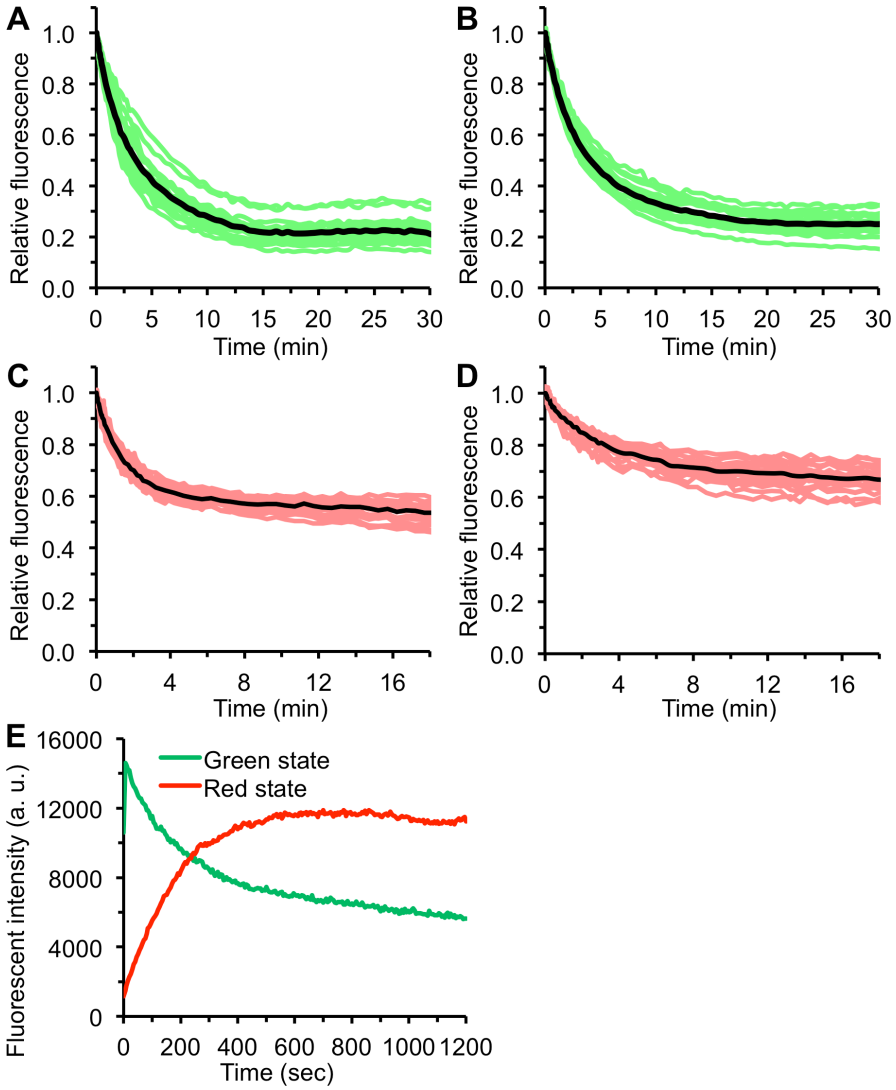

Figure S11. Photobleaching and photoconversion profiles for GR-GECOs. (A-D) Photobleaching of the green and red species of GR-GECO1.1 and GR-GECO1.2 targeted to the nucleus of HeLa cells. Illumination source is identical to that used to acquire the imaging data shown in Figure 3, Figure S10, and Movie S1. (A) Green species of GR-GECO1.1. (B) Green species of GR-GECO1.2. (C) Red species of GR-GECO1.1. (D) Red species of GR-GECO1.2. Each colored line is the trace of an individual nucleus, while the black line represents the average. (E) Representative photoconversion profile for a transfected HeLa cell expressing GR-GECO1.1, using the same photoactivation source used to acquire the imaging data shown in Figure 3, Figure S10, and Movie S1.

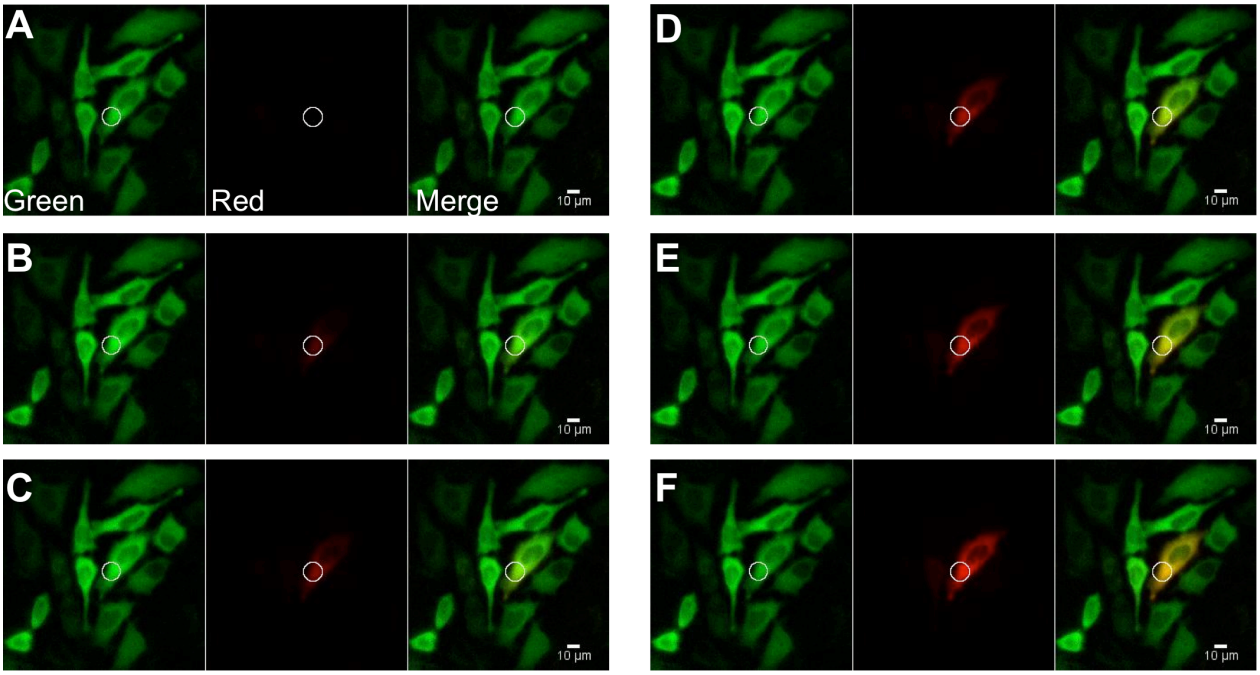

Figure S12. Highlighting a single cell in a densely transfected culture. (A) Before photoconversion. (B-F) Selected time points during photoconversion: (B) 25.5 sec; (C) 50.5 sec; (D) 75.5 sec; (E) 100.5 sec; and (F) 150.5 sec. For each panel, the left, center, and right images are the green fluorescence, red fluorescence, and merged channels, respectively. The white circle (diameter = 14.3 μm) represents the size and location of the 408 nm laser spot used for photoactivation.

Supporting Tables

Table S1. Properties of mMaple and its circularly permuted variants.

		λ_{exc} (nm)	λ_{em} (nm)	ε[a]	Φ	brightness[b]
green	mMaple	489	505	15	0.74	11
	cpmMaple193	489	505	18	0.80	14
	cpmMaple207	489	505	14	0.84	12
red	mMaple	566	583	30	0.56	17
	cpmMaple193	566	582	32	0.50	16
	cpmMaple207	566	582	29	0.53	15

[a]Unit of $mM^{-1} cm^{-1}$. [b]Product of ε and Φ in $mM^{-1} cm^{-1}$.

Table S2. Termini library of GR-GECOs.

Termini library	N-terminus position	C-terminus position	Library size	Brightness	Ca^{2+} response
1	146 147	141 142	64 × 64 = 4096	---	NA
2	145	143 144	32 × 64 = 2048	+	+
3	144 (V145Y[a])	143 144	32 × 64 = 2048	++	+
4	144 (V145Y[b])	145	32 × 32 = 1024	++	++

[a]A forward primer containing V145Y, a mutation decided from library 2, was used. [b]Mutation V145Y from now on will be named as +2Y while mutation E144G named as +1G since residues 144 and 145 also exists in the C terminus of cpmMaple.

Table S3. Genealogy and mutations in GR-GECOs.

	Mutations	Notes
GR-GECO0.1	cpmMaple (145Y-143W) + M68I/ N141H/ G145S/ K284M	Replace the cpGFP module with cpmMaple in G-GECO1.1. The result is a 3-part chimera composed of M13, cpmMaple and calmodulin.
GR-GECO0.2	GR-GECO0.1 + 62G/ 63Y/ V73aE/ D269N/ 302E/ 302aP	Best variant found in the termini libraries
GR-GECO0.3	GR-GECO0.2 + E61P/ N380W/ D381G	Best variant found in and semi-saturation libraries at position E61, R377, N380 and D381
GR-GECO0.5	GR-GECO0.3 + L60P/ K126E/ M146V/ T165A/ E197K/ Q244R/ R304H/ V430E/ N440S	Intermediate variant found during error-prone libraries and StEP libraries
GR-GECO1.1	GR-GECO0.5 + S88G/ T143A/ M158I/ A165T/ S276T/ T303V/ H304T/ K333E/ T413A/ T420A/ M427I	Variant displays good Ca^{2+} response at both green and red states in saturation libraries at position T303/R304
GR-GECO1.2	GR-GECO0.5 + S88G/ A165T/ I202V/ G262S/ T413A/ K418R/ E430V/ D434N	Variant displays best Ca^{2+} response at the red states in saturation libraries at position T303/R304

Table S4. Properties of GR-GECOs

Protein	Ca^{2+}	λ_{abs} with ε ($mM^{-1}·cm^{-1}$) in parenthesis		λ_{em} with Φ in parenthesis	Brightness[a]	pK_a	Intensity change with Ca^{2+}	K_d' (nM) for Ca^{2+} with Hill coefficient in parenthesis	(F_{Ca}-F_{EGTA})/F_{EGTA} in HeLa with number of trials in parenthesis[b]
GR-GECO0.5 (green)	−	386 (31)	490 (0.4)	509 (0.77)	0.3	9.4	2.9	199 (2.7)	2.7 ± 0.4 (15)
	+	383 (27)	490 (1.4)	507 (0.63)	0.9	8.8			
GR-GECO1.1 (green)	−	383 (29)	487 (1.5)	508 (0.70)	1.1	9.0	3.4	86 (2.0)	9.4 ± 1.7 (18)
	+	381 (27)	491 (5.7)	506(0.62)	3.5	8.5			
GR-GECO1.2 (green)	−	384 (30)	488 (1.1)	506 (0.65)	0.7	9.2	2.2	74 (1.7)	6.2 ± 1.3 (17)
	+	383 (29)	488 (2.2)	506 (0.71)	1.6	8.8			
GR-GECO0.5 (red)	−	558 (4.6)		582 (0.51)	2.3	8.2	2.8	96 (2.2)	2.7 ± 0.2 (15)
	+	557 (12.7)		584 (0.51)	6.5	7.5			
GR-GECO1.1 (red)	−	559 (5.5)		582 (0.46)	2.5	8.3	3.2	54 (2.6)	3.4 ± 0.6 (24)
	+	564 (14.1)		583 (0.57)	8.0	7.8			
GR-GECO1.2 (red)	−	558 (3.0)		581 (0.39)	1.2	8.4	4.6	90 (1.7)	5.1 ± 1.3 (51)
	+	558 (10.6)		582 (0.51)	5.4	7.5			

[a]Brightness is defined as the product of ε and Φ ($mM^{-1}·cm^{-1}$). [b]Cells were treated first with histamine, then with EGTA/ionomycin to give a minimum fluorescence F_{EGTA}, and finally with Ca^{2+}/ionomycin to give a maximum signal $F_{Ca.}$ Each trial represents an individual transfected cell on which systematic calibration experiments were performed.

Table S5. Kinetic characterization of GR-GECO1.1

Protein	k_{on} ($M^{-n}s^{-1}$)	k_{off} (s^{-1})	$n_{kinetic}$	$K_d'_{,kinetic}$ (nM)[a]	$K_d'_{,static}$ (nM)	n_{static}
GR-GECO1.1 (green)	1.50×10^{-5}	0.536	1.98	200	86	2.0
GR-GECO1.1 (red)	4.90×10^{-7}	0.582	2.56	235	54	2.6

[a] $K_d'_{,kinetic} = (k_{off}/k_{on})^{1/n}$

Supporting Movie Legends

Supporting Movie S1. Imaging of histamine-induced Ca^{2+} oscillations in a photoconverted HeLa cell expressing GR-GECO1.1. Green (left) and red (middle) fluorescence was imaged during photoconversion of a single cell and subsequent treatment with histamine to induce oscillations in the cytoplasmic Ca^{2+} concentration. The rightmost panel is a merged image of the green and red fluorescence images. Data is summarized in Figure S10.

Supporting Movie S2. Imaging of spontaneous Ca^{2+} oscillations in dissociated hippocampal neurons expressing GR-GECO1.2. A single neuron was partially photoconverted to the red fluorescent state. Data is summarized in Figure 4.

Primer List

cpGR_start_F: 5'-GGTGGCAGCGGTGGCATGGTGAGCAAGGGCGAGGA-3'

cpGR_end_R: 5'-GCCACCGCTGCCACCCTTGTACAGCTCGTCCATGCT-3'

cpGR207F2: 5'-TGTAGGTACCNNKTACAACAAGGTGAAGC-3'

cpGR207R2: 5'-ATTAGAATTCTCAACCGCCMNNGTCGTGGCTCAGGAT-3'

cpGR193F2: 5'-TGTAGGTACCNNKTTCGTGGACCACCG-3'

cpGR193R2: 5'-ATTATGAATTCTCAGCCACCMNNGTCGGGCAGCTTTAC-3'

cpGR145F2: 5'-AATAGGTACCNNKAGCACCGAGAAGATG-3'

cpGR145R2: 5'-ATTATGAATTCTCAGCCACCMNNCCAGCCCACGGTCCT-3'

cpGR140F: 5'-ATATGGTACCNNKGTGGGCTGGGAGGTCAG-3'

cpGR140R: 5'-GTTATGAATTCACCMNNCTTCTGCATCACGGGGCC-3'

cpGR143F: 5'-AATCAGGTACCNNKGAGGTCAGCACCGAGAAGATGTAC-3'

cpGR143R: 5'-GTTATGAATTCACCMNNCACGGTCCTCTTCTGCATCAC-3'

cpGR144F: 5'-AATCAGGTACCNNKGTCAGCACCGAGAAGATGTAC-3'

cpGR144R: 5'-GTTATGAATTCACCMNNGCCCACGGTCCTCTTCTG-3'

cp_M13F: 5'-GTTAATTATCTCGAGCAAGAGGCGCTGGCAGAA-3'

cp_M13R: 5'-CTTCTCGGTGCTMNNGGTACCCAGTGCCCCGGAGCT-3'

CaM_trunc_F: 5'-ACATGAATTCGACCAACTGACAGAAGAGCAGATTG-3'

cp_CaM_R: 5'-CCGGAAGCTTTCACTTTGCTGTCATCATTTGTAC-3'

XhoI_146X: 5'-GCAGGTGAGTAACTCGAGNNKACCGAAAAGATGTACGTGCG-3'

XhoI_147X: 5'-GCAGGTGAGTAACTCGAGNNKGAGAAGATGTACGTGCGGGAC-3'

XhoI-145X: 5'-GCAGGTGAGTAACTCGAGNNKAGCACAGAGAAGATCTACGTGCG-3'

XhoI_145YX: 5'-GCAGGTGAGTAACTCGAGNNKTACAGCACAGAGAAGATCTACGTGCG-3'

Mlu_141X: 5'-ATCACACGCGTMNNGGTCCTCTTCTGCATCACGGG-3'

Mlu_142X: 5'-AATGCACGCGTMNNCACGGTCCTCTTCTGCATCAC-3'

Mlu_143X: 5'-AAGTCACGCGTMNNGCCCACGGTCCTCTTCTGCATCAC-3'

Mlu_144X: 5'-AAGTCACGCGTMNNCCAGCCCACGGTCCTCTTCTGCATCAC-3'

Mlu145X: 5'-AAGTCACGCGTMNNTTCCCAGCCCACGGTCCTCTTCTG-3'

QC_E61: 5'-GAGCTATAGGTCGGCTGAGCTCACTCNNKNNKTACAGCACAGAGAAGATCTACGTGCG-3'

CaM_R377_fwd: 5’-ACGATGATGGCANNKAAAATGAAT-3’

GC-CaM_R377_fwd: 5’-ATTCATTTTMNNTGCCATCATCGT-3’

CaM_N380_fwd: 5’-GCAAGAAAAATGNNKNNKACAGACAGTGAA-3’

GC-CaM_N380_fwd: 5’-TTCACTGTCTGTMNNMNNCATTTTTCTTGC-3’

CaM_380F: 5'-CGATGGCAVBSAAAATGNNKNRSACAGACAGTGAAGAGGAAATTAGAGA-3'

CaM_380R: 5'-SYNMNNCATTTTSVBTGCCATCATCGTCAGGAACTCAGG-3'

XbaI_fwd: 5'-ACGCTTCTAGAGGTTCTCATCATCAT-3'

QC_TR_fwd: 5'-AAGAGGACCGTGGGCTGGGAACCTNNKNNKGACCAACTGACTGAAGAGCAGATC-3'

QC_GR_C+1: 5'-CTGGGAACCTGTTACGNNKGACCAACTGACTGAAG-3'

QC_GR_C+2: 5'-CTGGGAACCTGTTACGNNKNNKGACCAACTGACTGAAG-3’

GCaMP_FW_BamH1: 5'-GAGGATCCACCATGGTCGACTCATCACGTC-3’

GCaMP_RV_EcoR1: 5'-CGCGAATTCTTACTTCGCTGTCATCATTTGTAC-3’

QC_V203H: 5'-CCGACAACCACTACCTGAGCCATCAGTCCATACTTTCGAAAGA-3'

QC_V203X: 5'-TCTTTCGAAAGTATGGACTGMNNGCTCAGGTAGTGGTTGTCGG-3'

QC_E222Q: 5'-CATGGTCCTGCTGCAGTTCGTGACCGC-3'

paCaM_F1: 5'-GGCGCCCTGAAGAGCGAGVYGAAGVYSGGGVYGAGGCTGAAGGACGGCGG-3'

paCaM_F2: 5'-GCGCCTACATCGTCGACCGCAAGTTGGACATCGTGT-3'

paCaM_F3: 5'-CAGTTCATGTACGGCTCCVASGCCTACATTAAGCACCCA-3'

paCaM_SacI: 5'-TATTAGAGCTCACCCGTGVYSTCCGAGCGGAT-3'

paCaM_MluI: 5'-AGGCTACGCGTGACCAACT-3'

XhoI-GECO-Fwd 5'-ATGTGTGTAACTCGAGAATGGTCGACTCATCACGT-3'

GECO-BamH-Rev 5'-ATATTGGATCCTTTGCTGTCATCATTTGTACAAAC-3'

Supporting References

(1) Cubitt, A.B.; Heim, R.; Adams, S.R.; Boyd, A.E.; Gross, L.A.; Tsien, R.Y. *Trends Biochem. Sci.* **1995**, *20*, 448.

(2) van Thor, J.J.; Gensch, T.; Hellingwerf, K.J.; Johnson, L.N. *Nat. Struct. Biol.* **2002**, *9*, 37.

(3) van Thor, J.J. *Chem. Soc. Rev.* **2009**, *38*, 2935.

(4) Patterson, G.H.; Lippincott-Schwartz, J. *Science* **2002**, *297*, 1873.

(5) Wang, W.; Fang, H.; Groom, L.; Cheng, A.; Zhang, W.; Liu, J.; Wang, X.; Li, K.; Han, P.; Zheng, M.; Yin, J.; Wang, W.; Mattson, M.P.; Kao, J.P.; Lakatta, E.G.; Sheu, S.S.; Ouyang, K.; Chen, J.; Dirksen, R.T.; Cheng, H. *Cell* **2008**, *134*, 279.

(6) Tian, L.; Hires, S.A.; Mao, T.; Huber, D.; Chiappe, M.E.; Chalasani, S.H.; Petreanu, L.; Akerboom, J.; McKinney, S.A.; Schreiter, E.R.; Bargmann, C.I.; Jayaraman, V.; Svoboda, K.; Looger, L.L. *Nat. Methods* **2009**, *6*, 875.

(7) Henderson, J.N.; Gepshtein, R.; Heenan, J.R.; Kallio, K.; Huppert, D.; Remington, S.J. *J. Am. Chem. Soc.* **2009**, *131*, 4176.

(8) Bizzarri, R.; Serresi, M.; Cardarelli, F.; Abbruzzetti, S.; Campanini, B.; Viappiani, C.; Beltram, F. *J. Am. Chem. Soc.* **2010**, *132*, 85.

(9) Zhao, Y.; Araki, S.; Wu, J.; Teramoto, T.; Chang, Y.F.; Nakano, M.; Abdelfattah, A.S.; Fujiwara, M.; Ishihara, T.; Nagai, T.; Campbell, R.E. *Science* **2011**, *333*, 1888.

(10) Matz, M.V.; Fradkov, A.F.; Labas, Y.A.; Savitsky, A.P.; Zaraisky, A.G.; Markelov, M.L.; Lukyanov, S.A. *Nat. Biotechnol.* **1999**, *17*, 969.

(11) Subach, F.V.; Patterson, G.H.; Manley, S.; Gillette, J.M.; Lippincott-Schwartz, J.; Verkhusha, V.V. *Nat. Methods* **2009**, *6*, 153.

(12) Subach, F.V.; Malashkevich, V.N.; Zencheck, W.D.; Xiao, H.; Filonov, G.S.; Almo, S.C.; Verkhusha, V.V. *Proc. Natl. Acad. Sci. U. S. A.* **2009**, *106*, 21097.

(13) Fromant, M.; Blanquet, S.; Plateau, P. *Anal. Biochem.* **1995**, *224*, 347.

(14) Zhao, H.; Zha, W. *Nat. Protoc.* **2006**, *1*, 1865.

(15) Ai, H.; Henderson, J.N.; Remington, S.J.; Campbell, R.E. *Biochem. J.* **2006**, *400*, 531.

(16) Ward, W. W. Biochemical and physical properties of GFP In *Green fluorescent protein: Properties, applications, and protocols*; Chalfie, M., Kain, S. R. Eds.; Wiley: New York, 1998; pp. 45-75.

(17) Shaner, N.C.; Campbell, R.E.; Steinbach, P.A.; Giepmans, B.N.; Palmer, A.E.; Tsien, R.Y. *Nat. Biotechnol.* **2004**, *22*, 1567.

(18) Brannon, J.H.; Magde, D. *J. Phys. Chem.* **1978**, *82*, 705.

(19) Nienhaus, K.; Nienhaus, G.U.; Wiedenmann, J.; Nar, H. *Proc. Natl. Acad. Sci. U. S. A.* **2005**, *102*, 9156.

(20) Wang, Q.; Shui, B.; Kotlikoff, M.I.; Sondermann, H. *Structure* **2008**, *16*, 1817.

(21) McEvoy, A.L.; Hoi, H.; Bates, M.; Platonova, E.; Cranfill, P.J.; Davidson, M.W.; Ewers, H.; Liphardt, J.; Campbell, R.E. *PLoS ONE* **2012**, *7*, e51314.